CHAPTER THREE

3.0 DINDING SCHIST - PETROGRAPHY AND GEOLOGICAL STRUCTURES

3.1 Introduction

In the study area is exposed the lower part of the Dinding schist (Gobbett, 1964) and it is the objective of this chapter to describe the petrographic and structural features in them. During fieldwork, all bedrock exposures were described in detail as well as samples collected for petrographic studies. Reconnaissance field investigations were also carried out in several areas adjacent to Taman Ukay Perdana, including the Kuala Lumpur – Karak Highway, the Bentong area, Taman Melawati, Taman Melati, Bukit Antarabangsa, Wangsa Maju and the Zoo Negara area.

From more than 40 samples collected in the study area, eleven were selected for detailed laboratory studies. Selection criteria for these samples were that they should include as large a variety as possible, and that they should be representative ones. Thin sections were then prepared from four of the eleven samples for petrographic studies.

Measurements of the orientations of all geological structures present were also made during fieldwork, and their adequate interpretations were carried out. Pronounced structural features encountered include veins and joints. The flow structures include porphyroblasts and planar fabric such as foliation.

3.2 Field occurrence

The Dinding schist is exposed at several locations in the study area (Fig 3.1). Most exposures are massive and display a well developed foliation marked by the parallel alignment of thin (<5mm thick) dark greenish grey layers alternating with thicker, light greenish gray layers (Fig. 3.2). Slightly to highly weathered outcrops of the bedrock show the layering to be more pronounced with varying reddish brown colours due to alteration of original minerals as well as staining by secondary iron oxides and hydroxides (Fig. 3.3). The bedrock foliation generally strikes between 140° and 180° with some dips >40° towards the southwest (Fig.3.4). Late-phase granitic phenomena involving metasomatism is seen in bedrock exposures between Jalan UP 1/1 and Jalan UP 3/2 and marked by contortion of the original bedrock structure. Granite veins are also seen close to the metasomatised rocks, along Jalan UP 3/1, and in other areas of Taman Ukay Perdana. Minor cracks were also observed at most outcrops.

In several of the outcrops, the bedrock is seen to contain some small quartz and feldspar fragments (of up to 5 mm in size) that are sometimes elongated with a sub-parallel alignment. At most outcrops furthermore, the bedrock is seen to be cut by numerous thin quartz veins (<1 cm wide) of variable orientations that are often tightly folded and deformed. Rocks exposed in the study area have been classified as quartz-mica schists by several workers including Gobbett (1964), Mohamad *et al.* (1986), Komoo *et al.* (1985) and Nkpadobi and Raj (2008). In view of much evidence supporting an original pyroclastic bedrock, including the presence of bipyramidal quartz fragments and alternating textural layers, they would be better classified as meta-rhyolitic tuffs (Chuah, 1973).

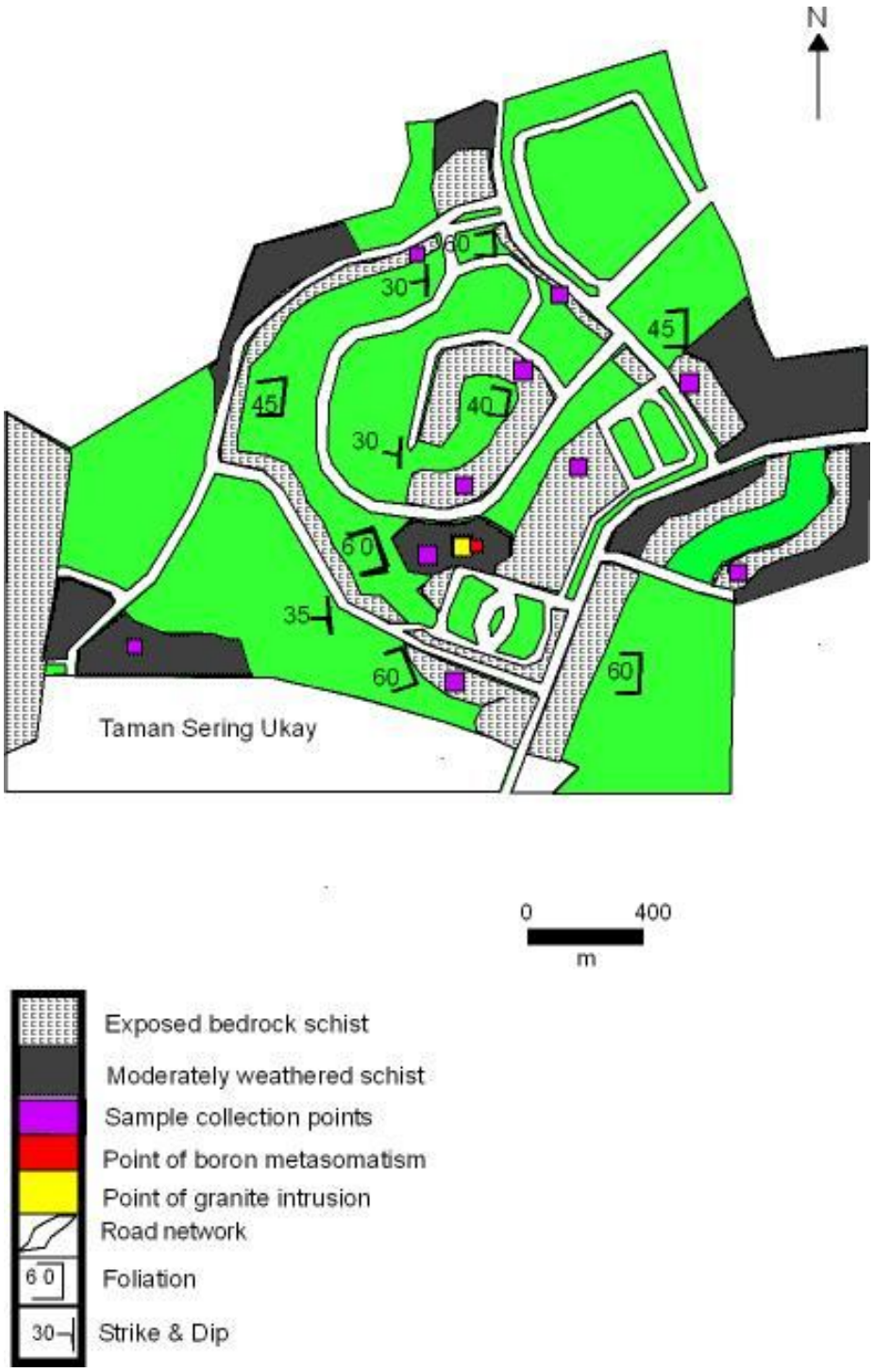

Fig. 3.1. Sample Location Map of Ukay Perdana area.

Fig. 3.2: Exposure of Dinding schist in Taman Ukay Perdana.

Fig. 3.3: Staining and alteration of original minerals in exposed bedrock in Jalan UP3.

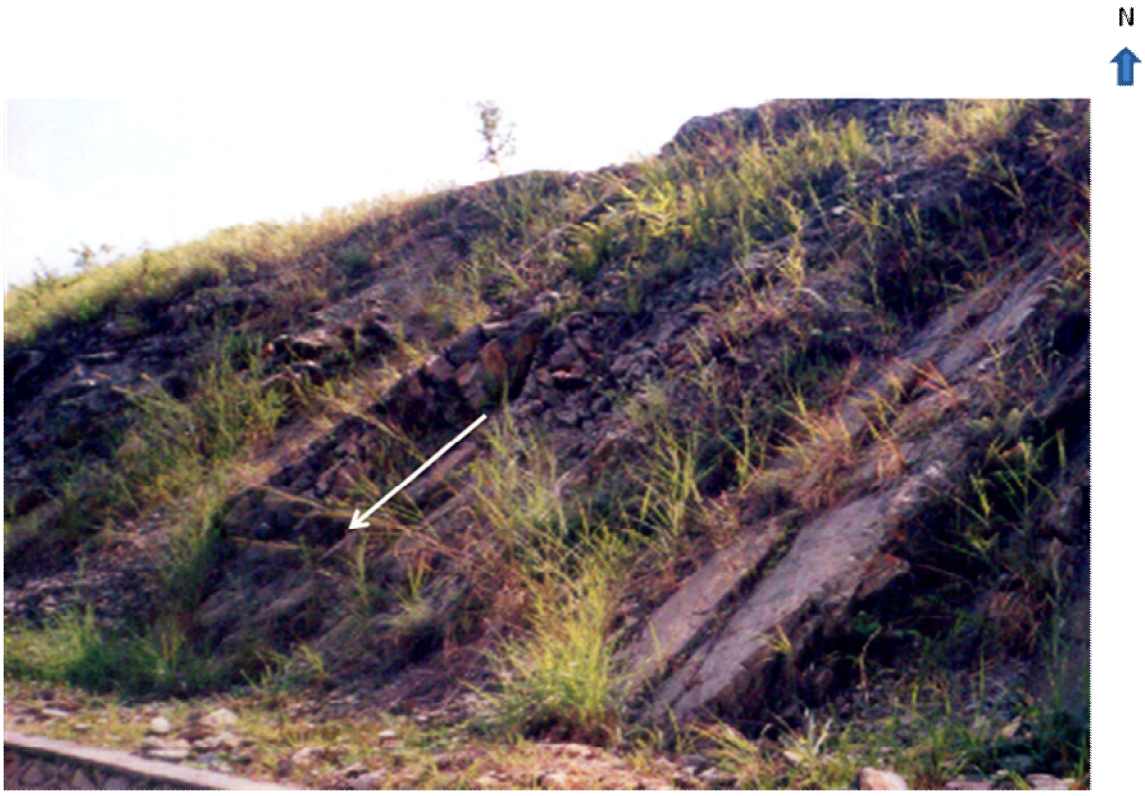

Fig. 3.4: Foliation trend of exposed bedrock in Jalan UP3.

3.3 Petrography of investigated rock materials

Studies of thin-sections have allowed determination of the petrography of the lower Dinding schist. In contrast to eruptive rocks which are classified in various logical ways on the basis of their mineral and chemical composition, metamorphic rocks do not yet have a clear universally accepted nomenclature. Metamorphic rock nomenclature uses structural or textural criteria, the nature of the rocks protolith (original rock from which the rock was derived) or the observed mineral assemblage. This is however, not totally rational and depends on local or regional usage. For this reason it is useful in all cases to describe the rock briefly, underlining its textural and mineralogical characteristics in precise terms (Kornprobst, 2002).

3.3.1 Sample UM/GLG/2005/A

The thin-section of this rock sample, collected at Jalan UP4 (Fig. 3.5), shows a predominance of muscovite and quartz with pronounced relic microcline and a few quartz porphyroblasts. Muscovite is the main silicate mineral present while microcline porphyroblasts are the least dominant and exhibit characteristic cross-hatched twinning (Fig. 3.6a, Fig. 3.6b, and Fig. 3.6c). This representative sample is best classified as a quartz-muscovite schist.

Fig. 3.5: Sample UM/GLG/2005/A collection point.

Figure 3.6a.: Photomicrograph of sample UM/GLG/2005/A showing irregular quartz porphyroblasts in fine grained matrix of quartz and muscovite.

Magnification.: 2.5x (Scale in left-hand corner is 0.3 mm long).

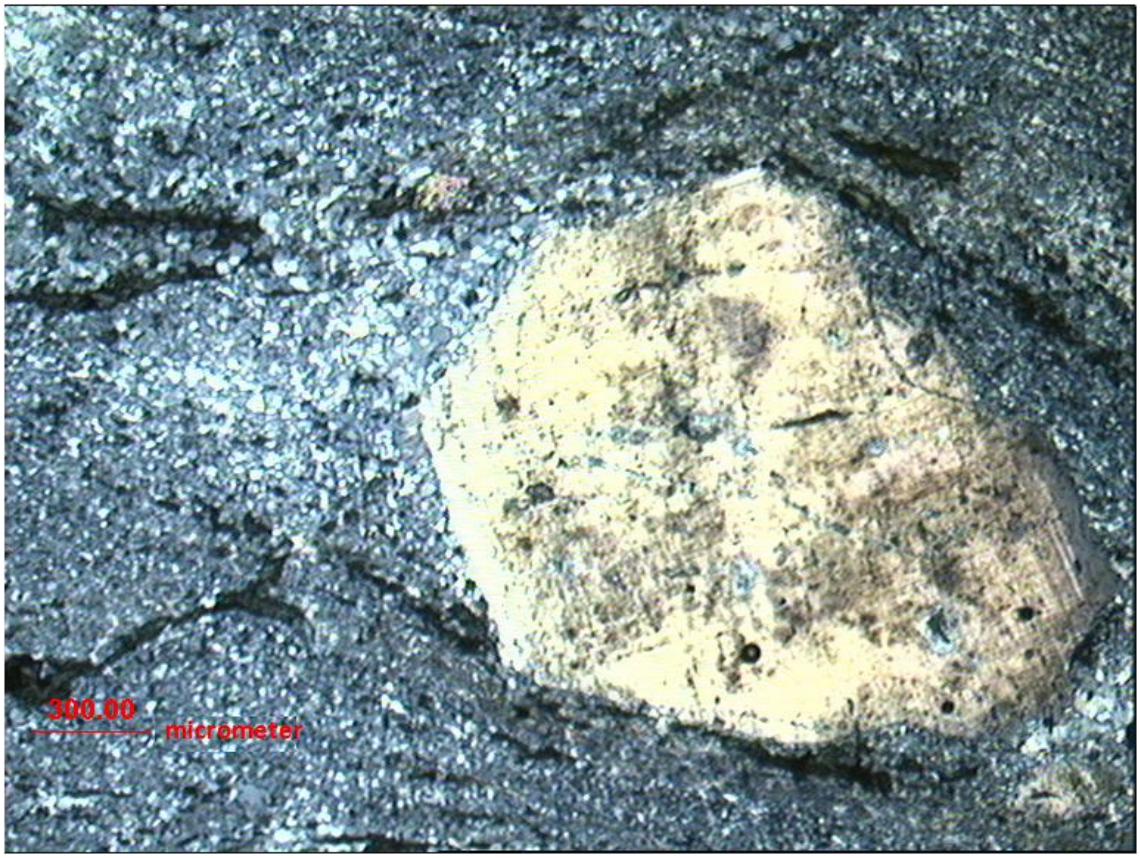

Figure 3.6b.: Photomicrograph of sample UM/GLG/2005/A showing relic microcline within matrix of fine grained quartz and muscovite.
Magnification.: 2.5x. (Scale in left-hand corner is 0.3 mm long).

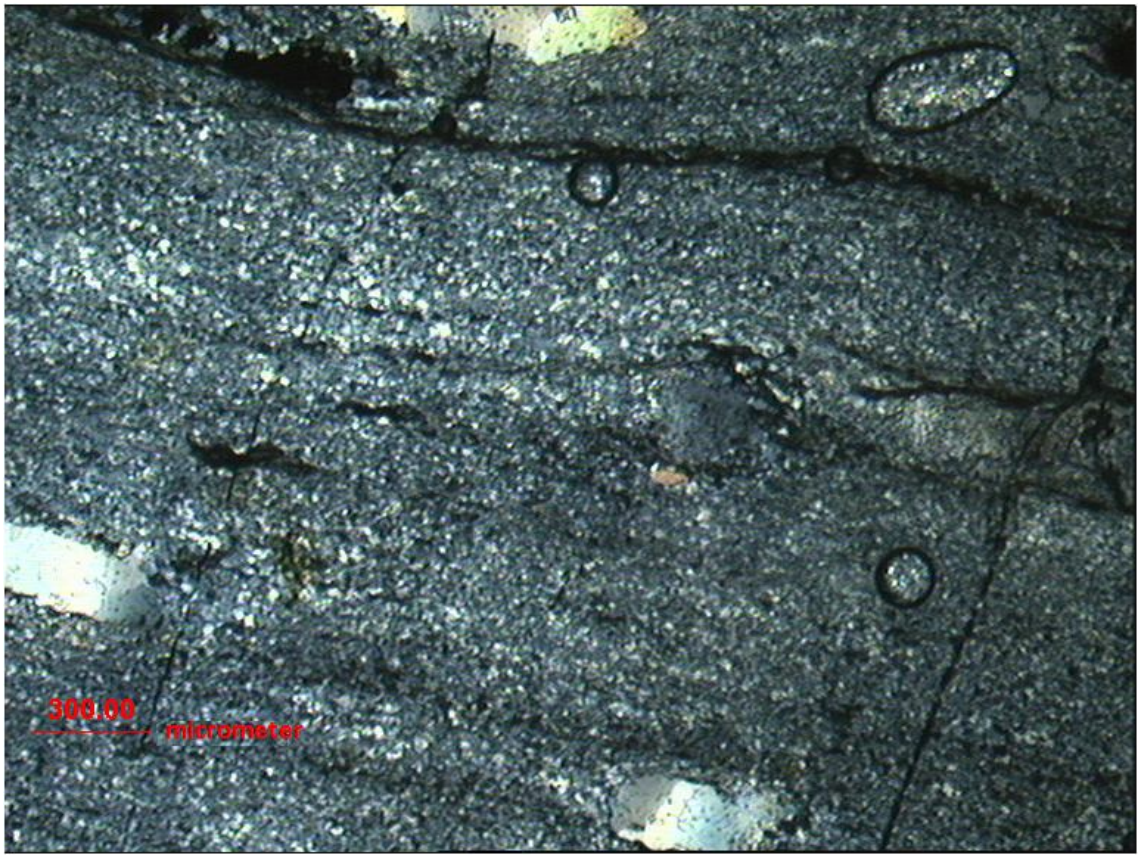

Figure 3.6c.: Photomicrograph of sample UM/GLG/2005/A showing foliation trend of the schistose rock.
Magnification.: 2.5x. (Scale in left-hand corner is 0.3 mm long).

3.3.2 Sample UM/GLG/2005/B

This thin section clearly shows all the different minerals constituting the rock with irregularly shaped quartz porphyroblasts seen as individual grains in an aligned matrix of alternating muscovite and fine grained quartz. Biotite occurs as small flakes. Photomicrographs of this thin-section are shown in Fig. 3.7a and Fig. 3.7b. The rock sample from which the thin-section was made is best termed a quartz-muscovite-biotite schist.

Figure 3.7a.: Photomicrograph of sample UM/GLG/2005/B showing quartz porphyroblast within an aligned matrix of fine grained quartz , muscovite and biotite.

Magnification.: 2.5x. (Scale in left-hand corner is 0.3 mm long).

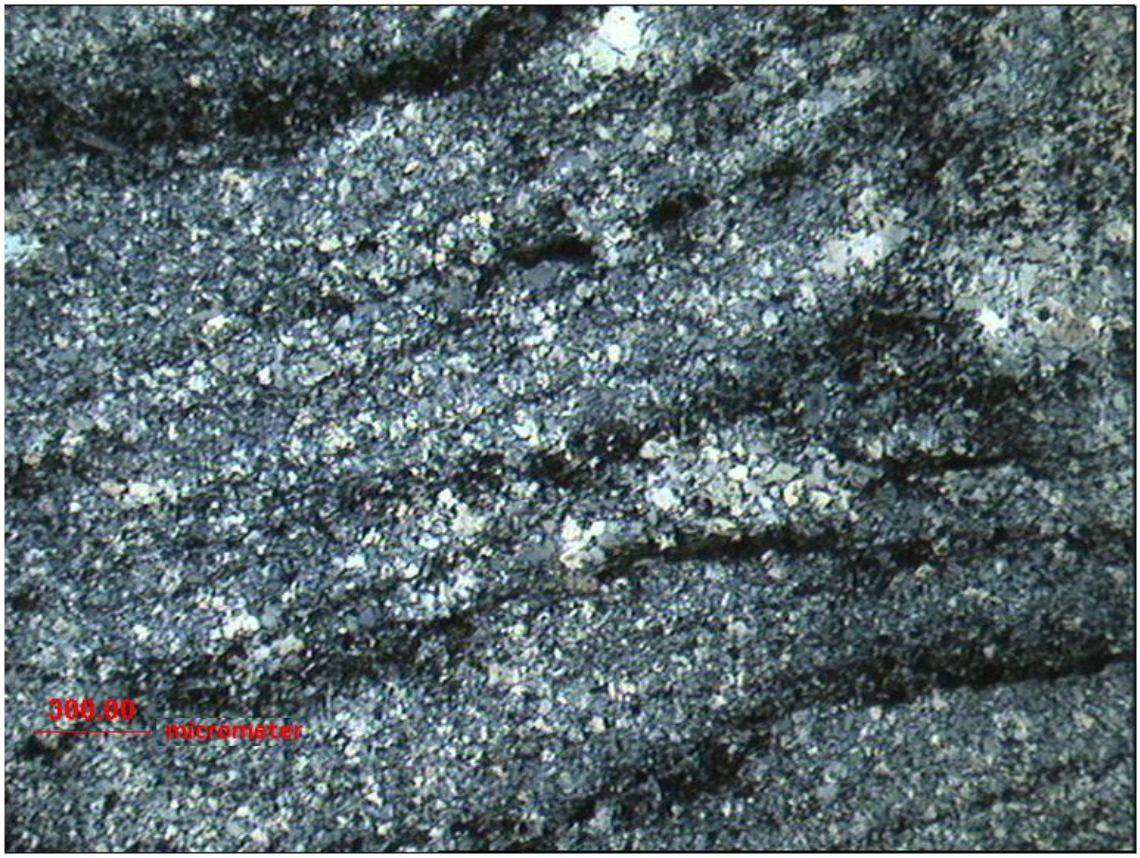

Figure 3.7b.: Photomicrograph of sample UM/GLG/2005/B showing the foliation trend of the schist.

Magnification.: 2.5x. (Scale in left-hand corner is 0.3 mm long).

3.3.3 Sample UM/GLG/2005/C

This thin-section was prepared from a rock sample collected at the same locality of the metasomatised bedrock. This sample comprises the granite that intruded into the older schist as a vein. The schist is twisted and contorted in places due to the intrusion. Photomicrographs of the thin-section under cross polarized light are seen in Fig. 3.8a, Fig. 3.8b, and Fig. 3.8c. Fig. 3.8b shows the granite/schist boundary, while only granite is seen in Fig. 3.8c. Muscovite and biotite are found within a matrix of fine grained quartz in the schistose part of the sample with microcline being the least dominant porphyroblast. Coarse grained quartz is the most dominant mineral in the granite.

Figure 3.8a.: Granite photomicrograph of sample UM/GLG/2005/C. The quartz is translucent with flecks of muscovite, biotite, and k-feldspars. Magnification. : 2.5x. (Scale in left-hand corner is 0.3 mm long).

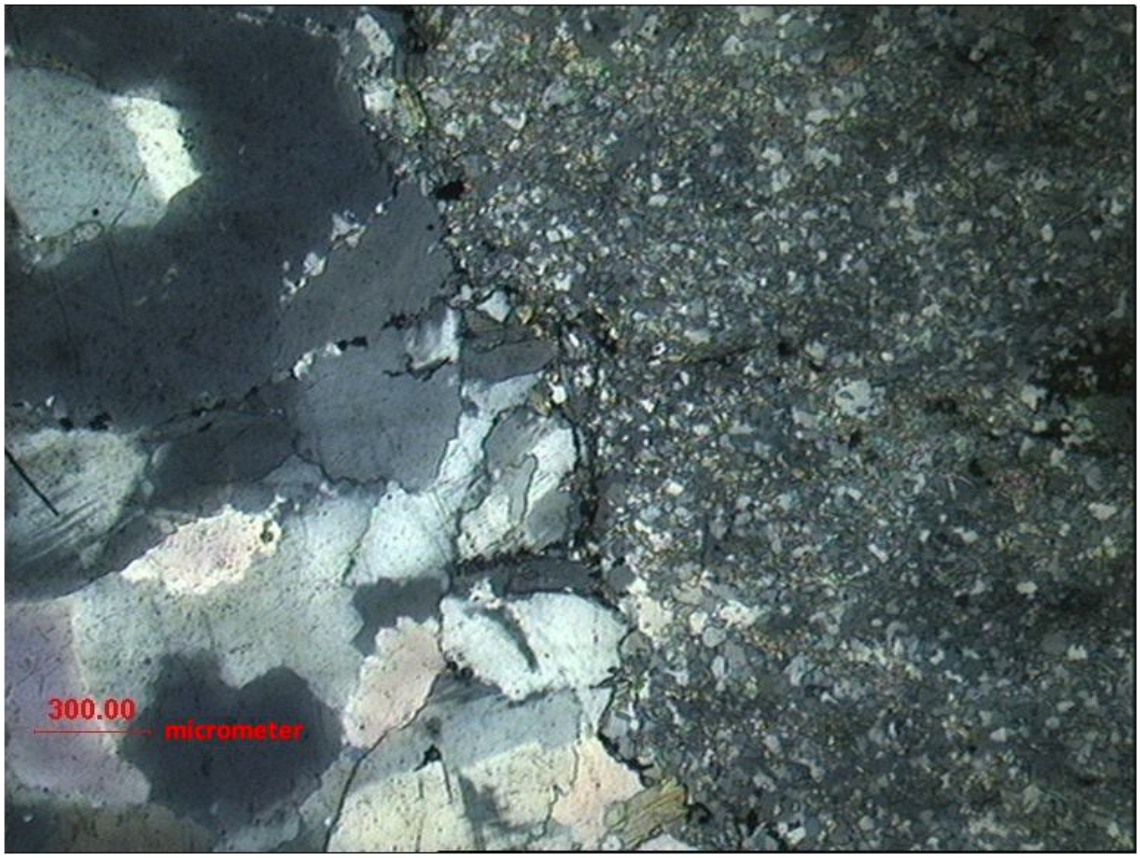

Figure 3.8b.: Photomicrograph of sample UM/GLG/2005/C showing granite/schist boundary.

Magnification.: 2.5x. (Scale in left-hand corner is 0.3 mm long).

Figure 3.8c.: Photomicrograph of sample UM/GLG/2005/C. The quartz and microcline porphyroblasts are seen as individual grains.
Magnification.: 2.5x. (Scale in left-hand corner is 0.3 mm long).

3.3.4 Sample UM/GLG/2005/D

The thin-section shows the original structures of this bedrock sample, collected at Vierra Ukay (Fig. 3.9) to have been partially obliterated. Quartz grains under cross polarized light show white and gray colours; the quartz porphyroblasts being of irregular shapes and seen within an aligned matrix of fine grained quartz, muscovite and biotite. Photomicrographs of the thin-section are seen in Fig. 3.10a and Fig. 3.10b.

Fig. 3.9: Sample UM/GLG/2005/D location point.

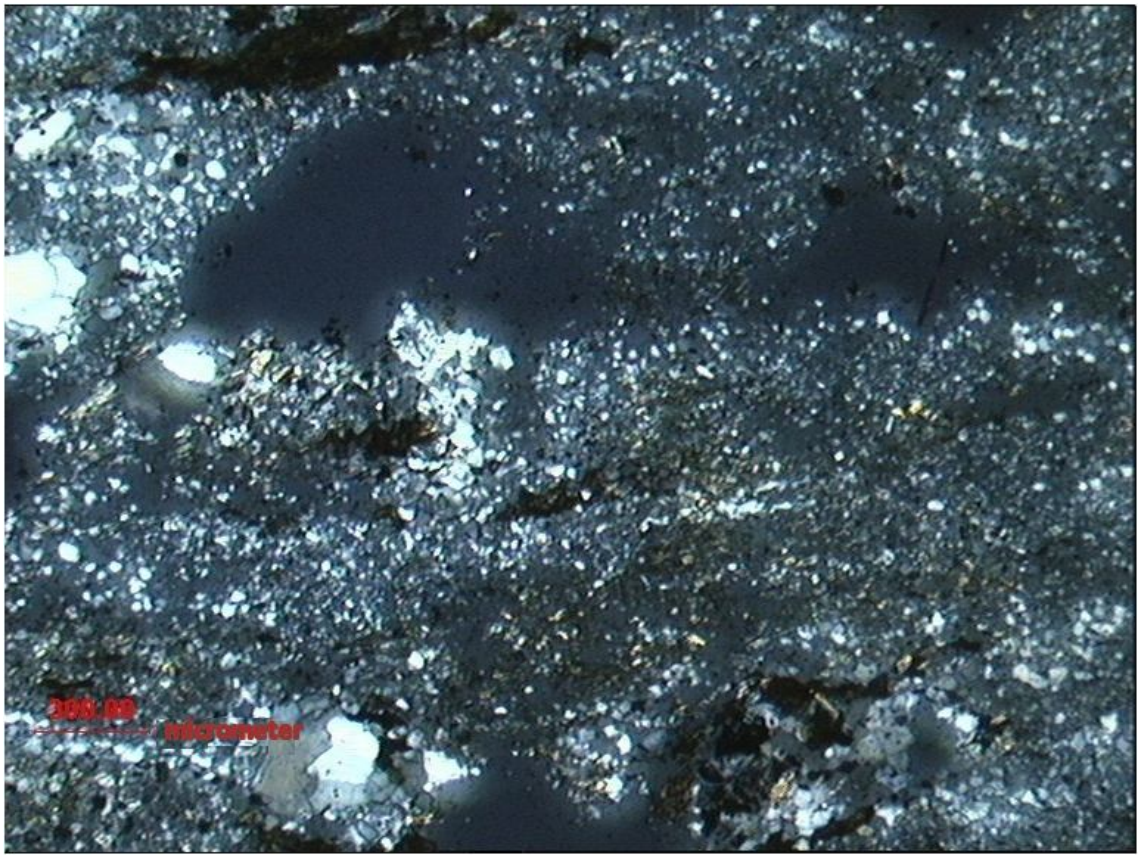

Figure 3.10a. Photomicrograph of sample UM/GLG/2005/D. The quartz porphyroblasts are seen within the fine grained quartz and muscovite with small flakes of albite. Magnification.: 2.5x. (Scale in left-hand corner is 0.3 mm long).

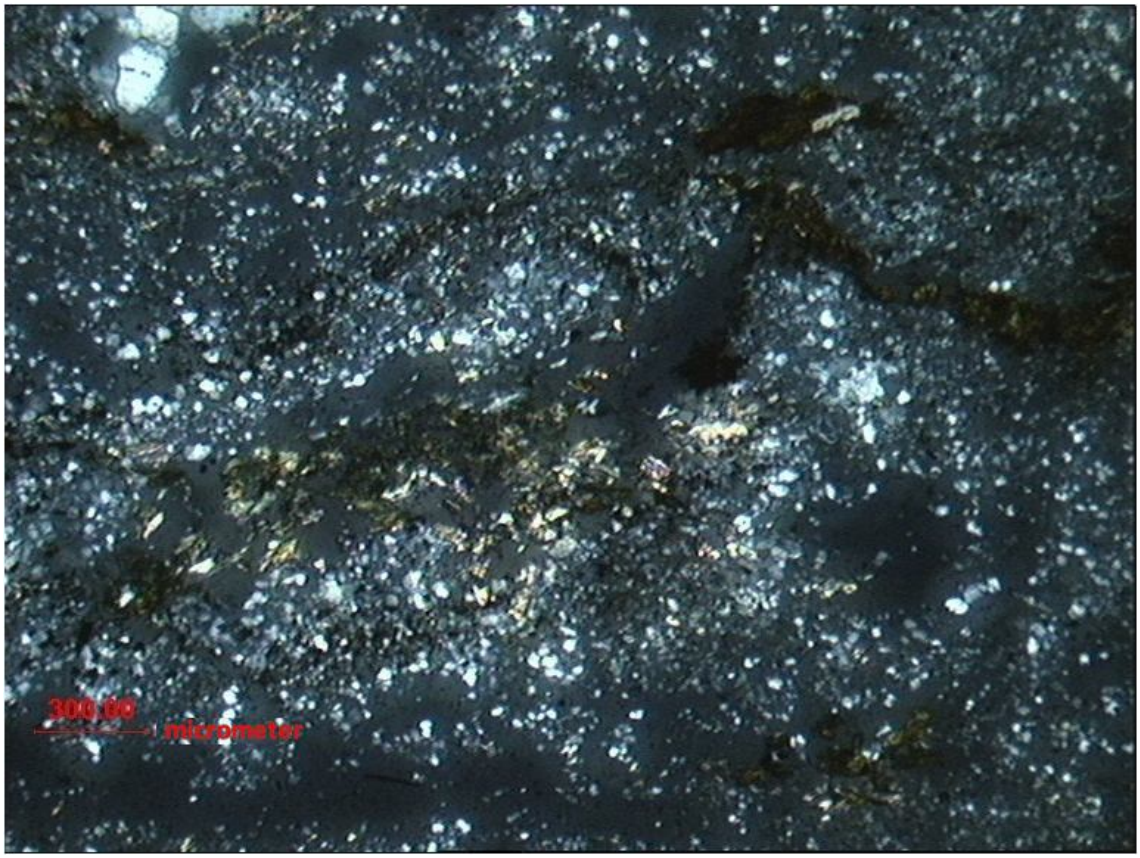

Figure 3.10b.: Photomicrograph of sample UM/GLG/2005/D showing the layered structure of the original rock. Magnification.: 2.5x.
(Scale in left-hand corner is 0.3 mm long).

3.3.5 Summary on Petrography

Evidence for intrusion of the granite into the Dinding schist is seen in the contorts nature of the foliation as well as the metasomatised bedrock. Mineralogical and structural changes are also evident in the weathered rock samples. The study of the thin-sections has confirmed the views of previous authors (Wong 1980; Khoo 1994; Raj, 2004), with the Dinding schist having a predominance of muscovite and quartz as well as relict microcline and small flakes of biotite. All of these features indicate that the Dinding schist in the study area is best termed a quartz-mica-schist.

3.4 Structures

3.4.1 Introduction

Ershov *et al* (1988) were of the opinion that structures are heterogeneities within rocks and are deformation products where deformation refers to processes that result in disturbances or dislocations within the original rocks. Three principal types of deformation mechanisms in rocks can be distinguished, i.e.

i) cataclastic flow

ii) crystalline plasticity, and

iii) diffusional flow/grain boundary sliding.

Rocks deform through one, or a combination of more than one, of these deformation mechanisms which are influenced by the physical and chemical environments of the rock during deformation and the application of forces on rock materials.

In the rocks of the study area, structures such as veins, joints and flow structures are found due to polyphase deformation. There is also super-positioning of minor structures either as a result of the sequential development of structures with progressive deformation during a single phase of deformation, or as a result of two or more separate tectonic events. Several factors are responsible for the products of deformation and include the orientation of shear and normal stresses, temperature, confining pressure, pressure of pore fluids and time duration.

3.4.2 Veins

Veins are extremely useful strain markers as they often enable the easy separation of different episodes of deformations. In the study area, granite veins are found in some exposures, especially between Jalan UP 1/1 and Jalan UP 3/2 (Fig.3.11). It is observed that the junction of the granite vein and the schist is distinctly seen, forming together a sloping surface uncovered by any fragment (Fig. 2.12). The granite veins show variable orientations and widths, though most veins show SE-NW and SW-NE strikes with widths of between 0.5 and 5 cm. These granite veins are evidence for the subsequent phase of the granite intrusion as well as contact metamorphism. These late Triassic to Jurassic granitic intrusions surrounding the Lower Palaeozoic rocks are broadly contemporaneous with, or younger than the second folding phase (Raj, 2004b).

Fig. 3.11: Schist outcrop along Jalan UP 3/2 with granite veins intrusion.

3.4.3 Joints

Joints are fractures of very small size and have been encountered in almost all bedrock outcrops in the study area. Though some of the joints may have resulted from blasting and excavation works for the slope cuts, most of them (especially with the NW-SE trend) probably have resulted from the late Triassic Indosinian orogeny.

The joints within the study area have widths of between 0.25 cm and 5 cm, and lengths of between 5 cm and 16cm and more. The longest joint, encountered at Jalan UP 3/1 is up to 8 m in length. A schematic diagram of the surfaces of the different types of joints encountered in the study area is shown in Fig. 3.12. Some of the joints are filled with clay materials, while others are open.

Most of the joints furthermore, generally dip towards the southwest, though some have very variable orientations especially those close to granite intrusions. The surfaces of the joints are slightly irregular with only a few surfaces being planar. Very few of the joint surfaces furthermore, are silky and smooth; most having shallow hollows and secondary fractures. Strikes and dips of joints within the study area are shown in Appendix 1, with the plots of poles for joint planes being shown in Fig. 3.13. A Rose diagram of the data contained in Appendix 1 is shown in Fig. 3.14 and is based on Table 3.1.

CLASS INTERVAL	FREQUENCY
0^{o} -30^{o}	16
31^{o} -60^{o}	11
61^{o} -90^{o}	7
91^{o} -120^{o}	11
121^{o} -150^{o}	16
151^{o} -180^{o}	23
TOTAL	**84**

Table 3.1. Data for trend of joints.

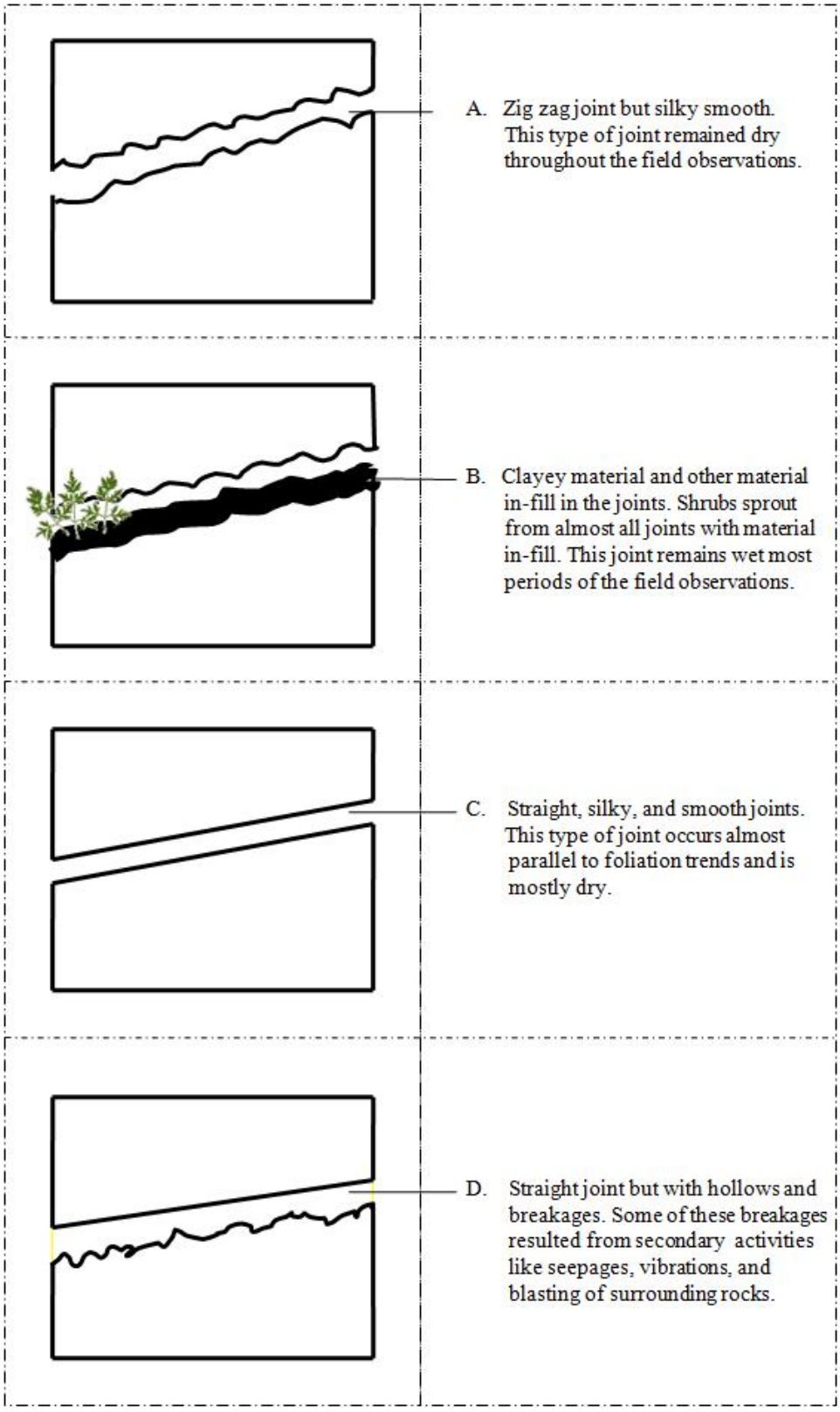

Fig. 3.12. Schematic sketch of various joint surfaces encountered in the study area.

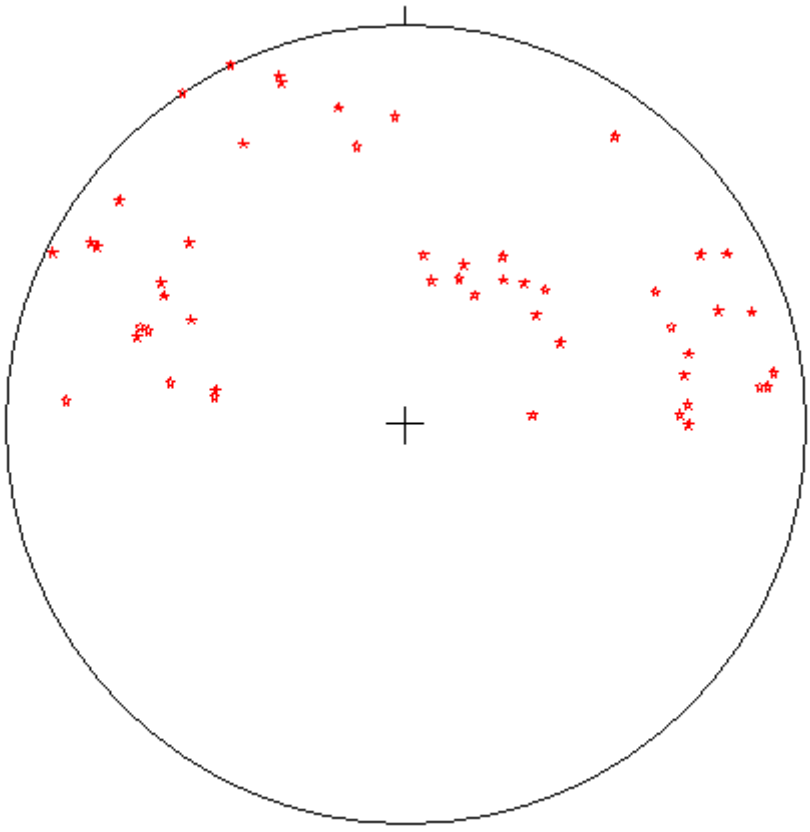

legend	
No. of Data	= 84
Mean principal Orientation	= 43/217
Mean Resultant direction	=42 -190
Mean Resultant length	= 0.67 (Variance =0.33)
Calculated girdle	=50/014
Calculated beta axis	=40-194

Fig. 3.13. Plot of Poles for joint planes

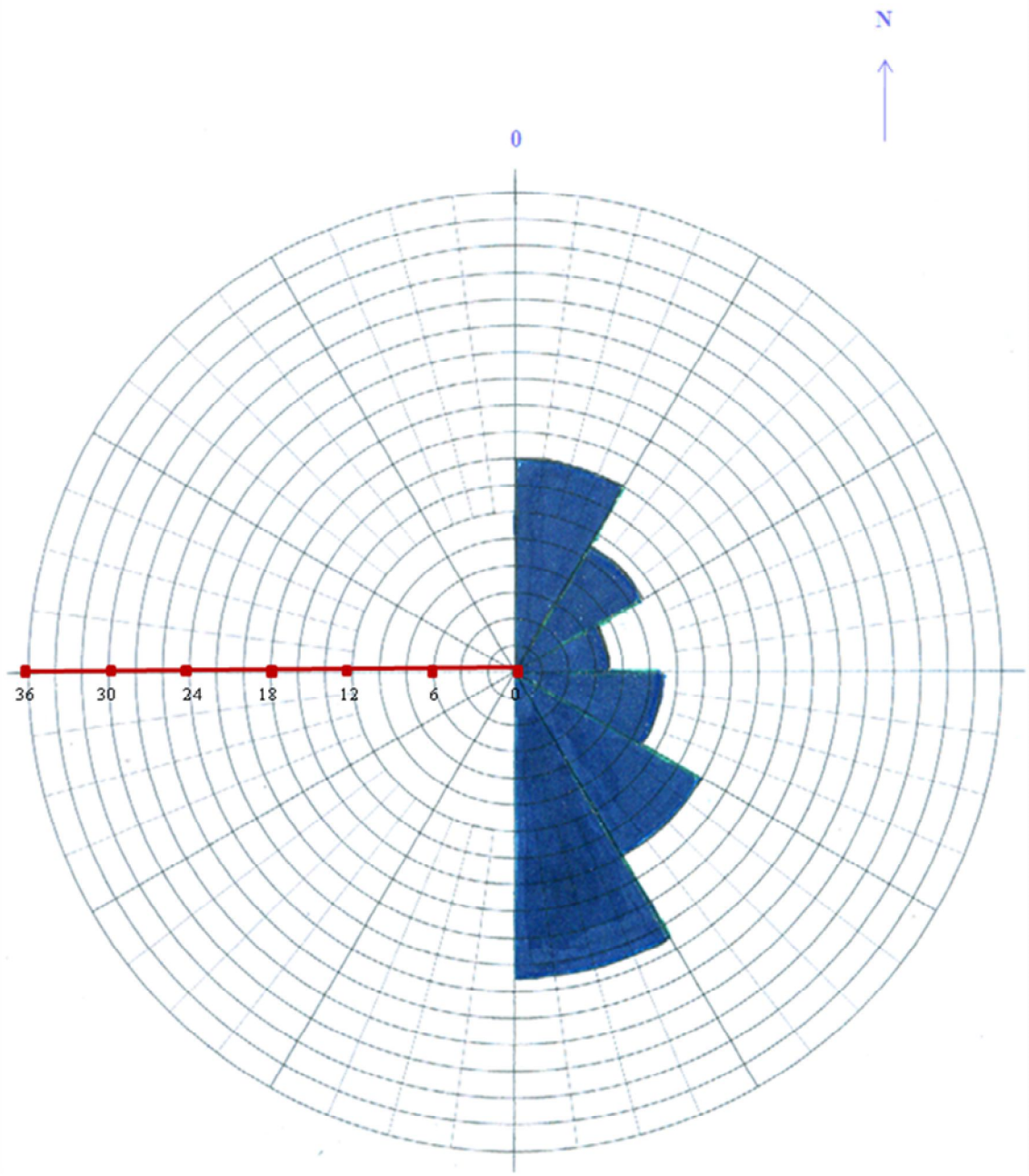

Fig. 3.14. Rose diagram showing joint orientation.

3.4.4 Flow structures

These are structures that develop within a rock as a consequence of the alignment of crystals and minerals during metamorphism and the intrusion of igneous bodies. Within the study area, porphyroblasts and planar fabric such as foliation were encountered. The size and shape of the quartz, microcline, and albite porphyroblasts encountered depend on the rate of nucleation and migration of chemical constituents to an appropriate site, causing the re-crystallization within the rock. Foliation is a planar fabric or preferred orientation with minerals being arranged in parallel alignment. Foliations in the study area are mostly due to deformation and re-crystallization and have a general SW trend. Chuah (1973) suggested that the foliation may be due to segregation during metamorphism, but may also be a relict structure representing heterogeneity in the original bedrock. Data on trends of foliation in the study area are shown in Appendix 2, whilst a rose diagram showing the trends of foliation is presented in Fig. 3.15 and is based on Table 3.2.

CLASS INTERVAL	FREQUENCY
0-30	3
31-60	4
61-90	6
91-120	4
121-150	11
151-180	9
TOTAL	**37**

Table 3.2: Data for trend of foliation.

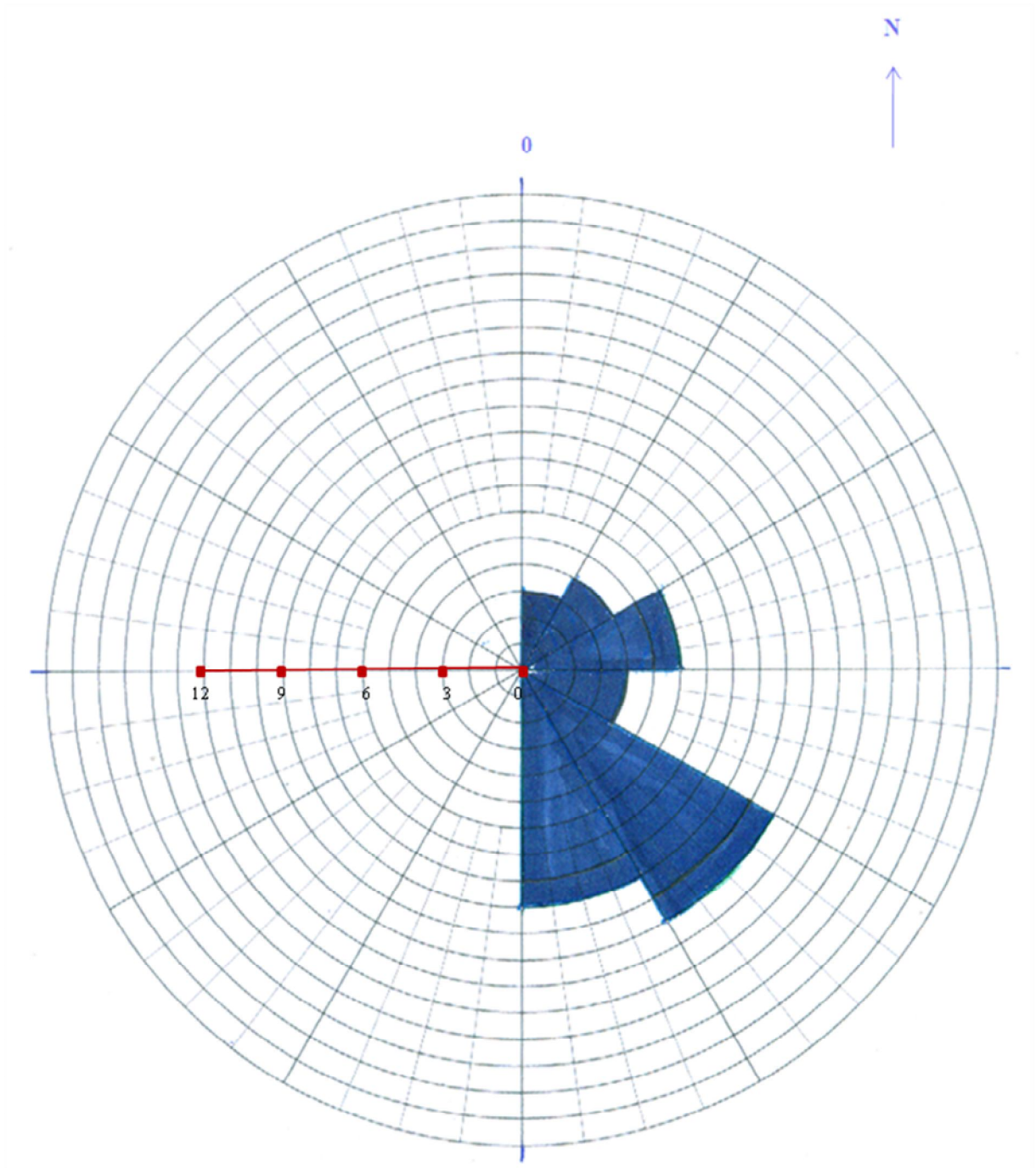

Figure 3.15. Rose diagram showing the trend of foliation.